Plenary paper

Antibody blockade or mutation of the fibrinogen γ-chain C-terminus is more effective in inhibiting murine arterial thrombus formation than complete absence of fibrinogen

Markéta Jiroušková, Igor Chereshnev, Heikki Väänänen, Jay L. Degen, and Barry S. Coller

An elevated plasma fibrinogen level is a risk factor for thrombotic cardiovascular disease, but which of fibrinogen's functions is responsible for the increased risk is unknown. To define better the contribution of fibrinogen to large vessel thrombus formation, we studied carotid artery thrombosis in wild-type mice, mice lacking fibrinogen (fbg$^{-/-}$), mice treated with 7E9 (a blocking antibody to the fibrinogen γ-chain C-terminus), and mice expressing a mutant fibrinogen (γΔ5) that lacks the γ-chain platelet-binding motif QAGDV. In control mice, thrombus formation resulted in occlusion in 8 ± 2 minutes (mean ± SD). In fbg$^{-/-}$ mice, thrombi grew to large sizes, but then they abruptly embolized, confirming previous observations by others in an arteriolar thrombus model. In contrast, mice treated with 7E9 and γΔ5 mice developed only small, nonocclusive mural thrombi and embolization was limited. These findings reveal that a fibrinogen antibody, 7E9, or a fibrinogen mutant retaining clotting function, can limit thrombus formation more effectively than the complete absence of fibrinogen. We hypothesize that the smaller thrombi in these animals result from the ability of fibrin to bind and sequester thrombin and/or the ability of the altered fibrinogen molecules, which cannot recruit platelets, to bind to and passivate the surface. (Blood. 2004;103:1995-2002)

© 2004 by The American Society of Hematology

Introduction

Abundant clinical and epidemiologic evidence indicates that fibrinogen contributes to both hemostasis and thrombosis,[1] but because fibrinogen has many different functions, it is less clear how each function contributes to these phenomena. Among the functions most likely to promote hemostasis and thrombosis are: (1) binding to platelet integrin $\alpha_{IIb}\beta_3$, thus supporting both platelet adhesion and aggregation; (2) binding to leukocyte (eg, $\alpha_M\beta_2$) and endothelial (eg, intercellular adhesion molecule 1 [ICAM-1]) receptors; (3) forming fibrin; (4) supporting fibrin cross-linking in concert with activated factor XIII (FXIIIa); (5) supporting clot retraction in concert with platelets; and (6) enhancing whole blood viscosity. The C-terminus of the fibrinogen γ chain is particularly important in fibrinogen function because it contains the platelet $\alpha_{IIb}\beta_3$ recognition sequence,[2,3] the FXIIIa cross-linking sites (Gln398 and Lys406),[4] and sites that may be important in fibrin monomer polymerization and lateral association.[5] Fibrinogen also has functions that may limit or antagonize hemostasis and thrombosis, including sequestering of thrombin via its binding to fibrin ("antithrombin I")[6,7] and facilitating thrombolysis via the binding of components of the fibrinolytic system to fibrin.[8] The ability of fibrinogen to both promote and limit hemostasis and thrombosis is reinforced by the observation that both bleeding and thrombosis have been reported in association with afibrinogenemia and some dysfibrinogenemias.[7,9]

Previous studies of mesenteric arteriolar thrombus formation in mice lacking fibrinogen (fbg$^{-/-}$) demonstrated the rapid development of large, nonocclusive thrombi that embolized repeatedly.[10] In mice lacking the $\alpha_{IIb}\beta_3$-binding site (QAGDV) in the C-terminus of the fibrinogen γ chain (γΔ5), thrombi also developed rapidly, but the thrombi were of intermediate stability (relative to wild-type and fbg$^{-/-}$ mice), demonstrating increased embolization compared to control but less than that observed in fbg$^{-/-}$ mice. Nevertheless, the thrombi were sufficiently stable to result in vascular occlusion at the site of injury in 88% of the injured arterioles.[11] Because the mesenteric arterioles that were studied are much smaller in diameter than human coronary arteries, we chose to study the carotid artery of mice, which better approximates the diameter of an atherosclerotic coronary artery. To assess thrombus formation and embolization in real time, we developed a novel imaging system of intravital videomicroscopy, which uses a fiberoptic light source and a surgical microscope. In addition to studying wild-type mice, fbg$^{-/-}$ mice, and γΔ5 mice, we also studied wild-type mice treated with the hamster monoclonal antibody 7E9.[12] We previously demonstrated that 7E9 binds to the C-terminus of the fibrinogen γ chain; inhibits platelet adhesion and aggregation, as well as platelet-mediated clot retraction; alters fibrin clot structure; inhibits FXIIIa-mediated fibrin cross-linking; and facilitates thrombolysis.[12,13]

Our observations of thrombus formation in the carotid arteries differ significantly from those obtained in mesenteric vessels,[10,11] but the disparate data can be reconciled on the basis of differences in blood vessel size. Most striking, however, is the paradoxical

The online version of the article contains a data supplement.

An Inside *Blood* analysis of this article appears in the front of this issue.

conclusion derived from our data that altering the C-terminus of the fibrinogen γ chain, either by the binding of antibody 7E9 or the deletion of the $\alpha_{IIb}\beta_3$-binding motif, is more effective in inhibiting arterial thrombus formation than complete absence of fibrinogen. This finding has important implications for understanding the pathophysiology of arterial thrombosis and devising therapeutic strategies.

Materials and methods

Animals used

C57Bl/6J mice were obtained from Jackson Laboratory (Bar Harbor, ME). C57Bl/6 inbred fibrinogen-deficient mice (Aα chain negative; fbg$^{-/-}$), their hemizygous littermate controls (fbg$^{+/-}$) that express about 75% of normal fibrinogen levels,[14] mice expressing mutant fibrinogen γΔ5 (lacking the platelet binding motif QADGV from the γ-chain C-terminus), and their wild-type littermate controls have been described previously.[14,15] Both female and male mice were tested, with a median age of 8.5 weeks (range, 7-15 weeks). In experiments where antibodies were injected, antifibrinogen (7E9 IgG; produced at National Cell Culture Center, Minneapolis, MN)[12,16] or control hamster IgG (ChromPure Syrian hamster IgG; Jackson ImmunoResearch Labs, West Grove, PA), both in sterile phosphate-buffered saline (PBS) at 11.3 mg/mL, were injected at 72 mg/kg through a tail vein 1 to 4 hours before inducing the carotid artery injury. All animal experiments followed protocols approved by the Institutional Animal Care and Use Committees at Rockefeller University and Mount Sinai School of Medicine.

Effect of 7E9 on bleeding time and platelet aggregation

Six C57Bl/6J mice were anesthetized with isoflurane and 50 μL blood was collected into EDTA (ethylenediaminetetraacetic acid) tubes (Microtainer Brand, Becton Dickinson, Franklin Lakes, NJ) by puncture of the retrobulbar venous plexus to obtain complete blood cell counts (CBCs) and baseline fibrinogen levels. The CBCs were measured using an ADVIA 120 (Bayer Diagnostics, Tarrytown, NY) set to measure mouse blood cells. The next day mice were injected with 7E9 or control hamster IgG. Bleeding time assays were performed 2 to 4 hours after the injection as described[17,18] by removing 2 mm from the end of the tail. The assay was terminated at 12 minutes if the tail was still bleeding. The mice were then anesthetized with isoflurane and blood was collected into both 3.8% sodium citrate (for fibrinogen and hamster IgG levels and for aggregation studies) and EDTA (for CBCs). Citrated blood was centrifuged at 140g at 22°C for 2 minutes, the platelet-rich plasma (PRP) was removed, 200 μL modified Tyrode buffer (138 mM NaCl, 2.7 mM KCl, 0.4 mM NaH$_2$PO$_4$, 12 mM NaHCO$_3$, 10 mM HEPES [N-2-hydroxyethylpiperazine-N'-2-ethanesulfonic acid], 5 mM glucose, 0.35% bovine serum albumin, pH 7.4) was added to the remaining blood and the cells were resuspended. Platelet-rich buffer (PRB) was obtained by centrifuging twice at 160g at 22°C for 2 minutes and added to the PRP. The remaining blood and buffer were centrifuged to obtain a mixture of plasma and Tyrode buffer for the adjustment of the platelet count (~600 000/μL) and as a blank for the aggregations studies. Aggregation of platelets in PRP/PRB induced by 10 μM adenosine diphosphate (ADP) was performed as described previously.[18]

Carotid artery thrombosis

Mice were anesthetized with isoflurane and maintained under inhalation anesthesia as described previously.[19] Prior to surgery, about 50 μL blood was obtained from the tail vein to assess baseline CBCs and plasma fibrinogen levels. Mouse body temperature was monitored with a rectal probe and maintained at 37 ± 1°C with a halogen lamp (type EPZ; Sylvania, New York, NY) placed about 30 cm from the mouse and aimed at the trunk. Surgery was performed with the aid of a surgical stereomicroscope (Carl Zeiss, Thornwood, NY), using magnifications of × 10 to × 20. The right common carotid artery was dissected free of surrounding tissue and then a Doppler flow probe (no. 0.5VB307; Transonic Systems, Ithaca,

NY), connected to a flow meter (T106; Transonic Systems), was placed on the carotid artery proximal to the bifurcation. The artery and the probe were covered with lubricating jelly (mixed 3:2 with normal saline) and the position of the probe was adjusted so that it displayed the highest blood flow rate. Blood flow was then monitored continuously throughout the procedure. To visualize thrombus formation, a transilluminator was positioned proximal to the flow probe with illumination coming from below (Figure 1). The transilluminator light guide consisted of 0.4-mm thick clear polycarbonate plastic strip, 47 mm long, 6 mm wide at the input end and 3.2 mm wide at the output end. The output end was sharply bent and cut on bias so that the cut surface pointed toward the top side of the light guide and the strip was bent slightly to make it fit under the artery. Front and back surfaces were covered with reflective adhesive tape (Scotch 850; 3M, St Paul, MN) and the top surface was covered close to the tip with matte black photo grade masking tape (Pearl Paint, Fort Lauderdale, FL) to reduce light reflections. Light to the light guide was provided by 5-mm diameter Lucite rod attached to the output of a fiber optic illuminator (Twinbeam-151X; Applied Fiberoptics, Southbridge, MA). Video recording was achieved by replacing one eyepiece of the surgical microscope with a miniature video camera (ProVideo CVC-514; CSI/SPECO, Amityville, NY) attached to a Sony GVD-300 Mini-DV video recorder (Sony Corp of America, Park Ridge, NJ).

After the optimal positioning of the flow probe and the illuminator was achieved, the lubricating jelly covering the flow probe was aspirated and the site was rinsed with normal saline. The exposed artery and surrounding tissue were dried with absorbing material. Injury was induced by placing filter paper (Whatman no. 1; 1 × 2 mm) saturated with 20% FeCl$_3$ on the illuminated segment of the carotid artery.[20] The filter paper was pressed to the vessel wall every 45 seconds with tweezers to secure its position on the vessel. After 3 minutes, the filter paper was removed and artery was covered with lubricating jelly. Blood flow and thrombus formation were then evaluated for 30 minutes. The time to occlusion was defined as the time from the application of FeCl$_3$ until the flow decreased by more than 90% of the original flow for longer then 30 seconds. After 30 minutes, the jelly was aspirated and the site of the injury washed with normal saline. Probes were then removed and blood obtained from the right ventricle into a syringe containing 6 μL 40% sodium citrate for further analysis of CBCs and plasma fibrinogen and hamster IgG levels. While the mouse was still under anesthesia, perfusion was performed with 10 mL 4% paraformaldehyde in PBS and the injured carotid artery, and in some cases the brain, were collected for electron microscopy and histology.

Histology, immunohistochemistry, and electron microscopy

Carotid arteries and brains were fixed overnight in 4% paraformaldehyde in PBS and then embedded, sectioned, and either stained with hematoxylin-eosin or processed for immunohistochemistry as described previously.[19] Platelets were identified with a rabbit antimouse thrombocyte polyclonal antibody (Inter-Cell Technologies, Hopewell, NJ).
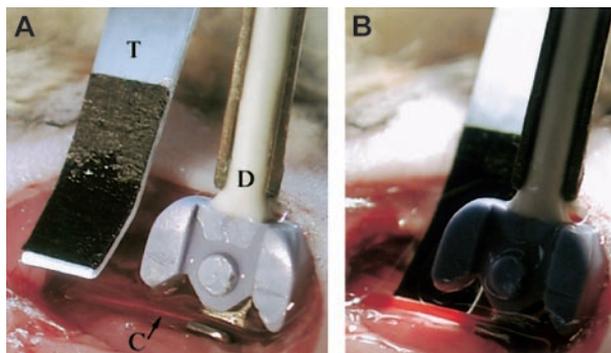

Figure 1. Transillumination of dissected carotid artery for intravital videomicroscopy. (A) The Doppler flow probe (labeled D) is positioned proximal to the bifurcation of the carotid artery (labeled C), with the artery in the flow probe's groove. The transilluminator (labeled T) is placed along side the artery, proximal to the flow probe so that the vessel is transilluminated from below (B).
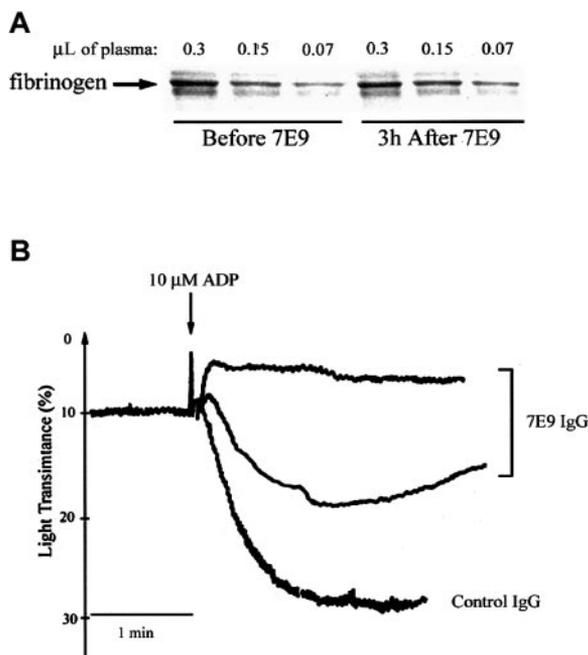
Figure 2. Administration of 7E9 in vivo does not affect plasma fibrinogen levels and inhibits platelet aggregation ex vivo 3 hours after injection. (A) Proteins in citrated mouse plasma obtained from the animal before and 3 hours after the injection of 7E9 IgG were separated on sodium dodecyl sulfate–polyacrylamide gel electrophoresis (SDS-PAGE) and transferred to polyvinylidene difluoride (PVDF) membrane; fibrinogen was then immunoblotted using an HRP-conjugated polyclonal rabbit antibody to human fibrinogen. (B) ADP-induced (10 μM) platelet aggregation 2 to 4 hours after the injection of control hamster IgG or 7E9 IgG. The upper tracing is representative of the results in 2 separate animals.

Immunoblot analysis

Citrated plasma prepared from the blood of the animals before and after surgery was analyzed for plasma fibrinogen and hamster IgG by immunoblotting. Relative fibrinogen plasma levels were estimated from the intensity of staining using a series of plasma dilutions. Fibrinogen was detected with a horseradish peroxidase (HRP)–conjugated rabbit antihuman fibrinogen polyclonal antibody (1:2000 dilution; Dako, Carpinteria, CA); hamster antibody 7E9 and control hamster IgG were detected with biotin-conjugated mouse anti-Armenian and anti-Syrian hamster monoclonal antibody (1:1000 dilution; PharMingen, San Diego, CA), followed by HRP-conjugated streptavidin (1:2500 dilution; Amersham Life Sciences, Little Chalfont, United Kingdom). Immunoblots were developed using a diaminobenzidine (DAB) peroxidase substrate kit (Vector Laboratories, Burlingame, CA).

Statistical analysis

Results are expressed as mean $\pm$ SD. Thrombosis data were analyzed using Exact 2-tail Cochran Armitage Trend test. Other results were analyzed using one-way ANOVA test or Student t test; P less than .05 was considered significant.

Results

Effects of control hamster IgG and 7E9 IgG on bleeding time, blood counts, plasma fibrinogen, and platelet aggregation

The mean bleeding time in the mice injected with the control hamster antibody was 1.2 ± 0.3 minutes ($\pm$ SD, n = 3). The bleeding times in 2 of 3 mice receiving 7E9 were more than 12 minutes; the third mouse stopped bleeding transiently at 5 minutes, but then started again 20 seconds later and continued until 12

minutes, when the experiment was terminated. Neither the control antibody nor 7E9 had a significant effect on blood counts (data not shown) or plasma fibrinogen levels (Figure 2A) compared to the baseline levels obtained the day before the injections. Platelet aggregation induced by 10 μM ADP was abolished in 2 mice treated with 7E9 and partially inhibited in the third one (initial slope inhibited by 50%; Figure 2B).

Carotid artery thrombosis

Control mice. Control animal group consisted of (1) normal C57Bl/6J (n = 2); (2) normal C57Bl/6J mice injected with control hamster IgG (n = 4); (3) C57Bl/6J-inbred fbg$^{+/-}$ mice (littermate hemizygous controls for fbg$^{-/-}$ animals; n = 6); and (4) C75Bl/6J-inbred wild-type littermates for γΔ5 mice (n = 2). These animals were ultimately analyzed as a single group because there were no significant differences in the time to carotid artery occlusion among the different groups (Table 1; $P = .88$). Blood flow through the carotid arteries of control mice was 1.4 ± 0.3 mL/min before FeCl$_3$ injury and 1.5 ± 0.4 mL/min immediately after the injury. Figure 3A shows a carotid artery blood flow recording from a mouse treated with control hamster IgG. This animal's response was typical of the responses of all of the controls. Visible thrombus formation began at the site of the injury immediately after the removal of FeCl$_3$-saturated filter paper (Figure 4; see also Supplemental Video 1, available on the *Blood* website and accessible through the Supplemental Videos link at the top of the online article). A compact and stable occlusive thrombus formed at the site of the injury 7.2 minutes after the initiation of the FeCl$_3$ injury in this control mouse (Figure 3A). For the entire group occlusion occurred after 8 ± 2 minutes (Table 1). Electron microscopy and histologic analysis revealed similar findings in all the control animals, with compact thrombi filling the entire lumen of the vessel (Figures 5-6). Only minimal embolization was observed visually through the surgical microscope. Histologic assessment of brain vasculature in 2 control fbg$^{+/-}$ animals demonstrated only rare emboli occluding small blood vessels (Figure 7). Thrombus formation did not result in a significant change in systemic platelet count ($1100 \pm 300 \times 10^3/\mu$L before, $1000 \pm 300 \times 10^3/\mu$L after the procedure).

Fibrinogen-deficient mice. As with the control mice, platelets began to deposit at the site of injury shortly after the removal of FeCl$_3$-saturated filter paper, but in contrast to the control animals extensive embolization was observed (Supplemental Video 2 contains details), with small platelet aggregates constantly detaching, rolling, and translocating from the growing surface of the thrombi. Thrombi eventually grew large, but were highly unstable and periodically embolized downstream. The embolization was so extensive that in 3 of 7 fbg$^{-/-}$ mice blood flow ultimately stopped as a consequence of the occlusion of the downstream circulation (Table 2). Figure 3 shows 2 typical blood flow recordings from

Table 1. Time to more than 90% reduction in blood flow after the application of FeCl$_3$ in control animals

Control group	Time to thrombosis, min, mean $\pm$ SD	No. of mice
C57Bl/6J	7*	2
Control hamster IgG	8 ± 2	4
Fbg$^{+/-}$	9 ± 2	6
γΔ5$^{+/+}$	7*	2
All controls	8 ± 2	14

* indicates the mean of 2 values.

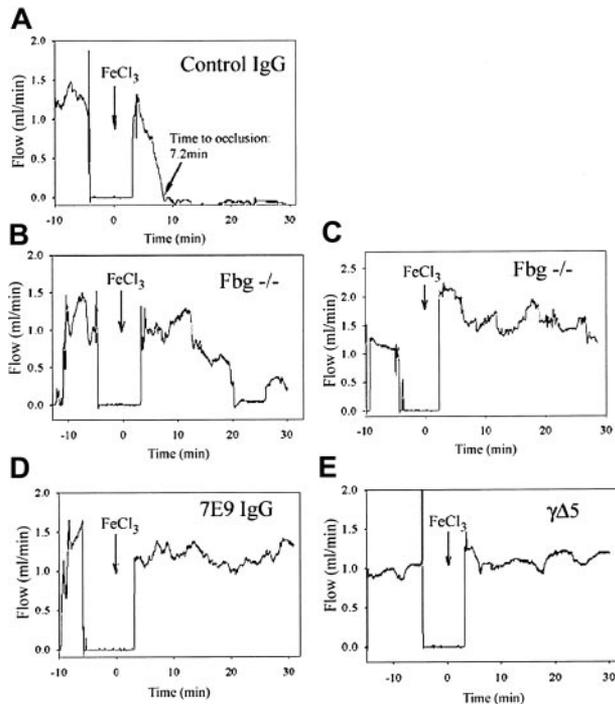**Figure 3. Compared to control mice, fbg$^{-/-}$ mice form unstable thrombi, and both 7E9-treated and γΔ5 mice form small mural thrombi.** Representative recordings of blood flow through the carotid artery before and after FeCl$_3$ injury in mice from each group. Blood flow through the carotid artery was recorded using a Doppler flow probe. Just before the injury, the lubricating jelly covering the probe was aspirated and then the site was rinsed with normal saline and dried. As a result, no blood flow was recorded during this time interval. Injury was induced by application of FeCl$_3$ (arrow; time 0) for 3 minutes, after which the artery was covered with lubricating jelly and flow was continuously recorded for 30 minutes. (A) A control animal that developed an occlusive thrombus at 7.2 minutes. Note that the blood flow remained dramatically reduced thereafter. (B-C) Results from 2 representative fbg$^{-/-}$ mice. The animal in panel B had multiple abrupt episodes of increased carotid blood flow corresponding to extensive embolization. Even after a sustained period of virtually no blood flow, at about 25 minutes embolization recurred and was associated with an increase in blood flow. The animal in panel C did not develop occlusive thrombus during the observation time period due to repeated embolization. (D-E) Neither the 7E9-treated mouse (D) nor the γΔ5 mouse (E) developed an occlusive thrombus during the 30-minute period.

fbg$^{-/-}$ mice. In the first recording (Figure 3B), corresponding to the animal whose carotid artery is shown in Figure 4 (and Supplemental Video 2), the injured carotid artery occluded at 20 minutes after the FeCl$_3$ application. Occlusion at the site of injury was followed by abrupt peeling of the thrombus from its attachment to the vessel wall and nearly complete embolization of the entire thrombus (Figure 4; video B). This embolization was not accompanied by return of blood flow, however, because the embolus was large enough to occlude the distal circulation and sufficient to reduce the blood flow at the more proximal site of injury. The second blood flow recording of a fbg$^{-/-}$ mouse further illustrates the repeated embolization of large thrombi as documented by the cyclical changes in blood flow (Figure 3C). However, in this animal neither the thrombi at the site of the injury nor the distal emboli caused a marked reduction in blood flow. The platelet counts in fbg$^{-/-}$ mice at the end of the experiment were slightly, but significantly, lower than at the beginning ($1300 \pm 200 \times 10^3/\mu$L before, $1100 \pm 400 \times 10^3/\mu$L after; n = 7, P = .049). Scanning electron microscopy and histology revealed that the thrombi formed in the injured arteries were very loose, not as compact as the ones formed in control mice, and contained large pores (Figures 5-6). Consistent with the recurring release of platelet aggregates from injured carotids in fbg$^{-/-}$ mice, histologic assessment of the brains of 3
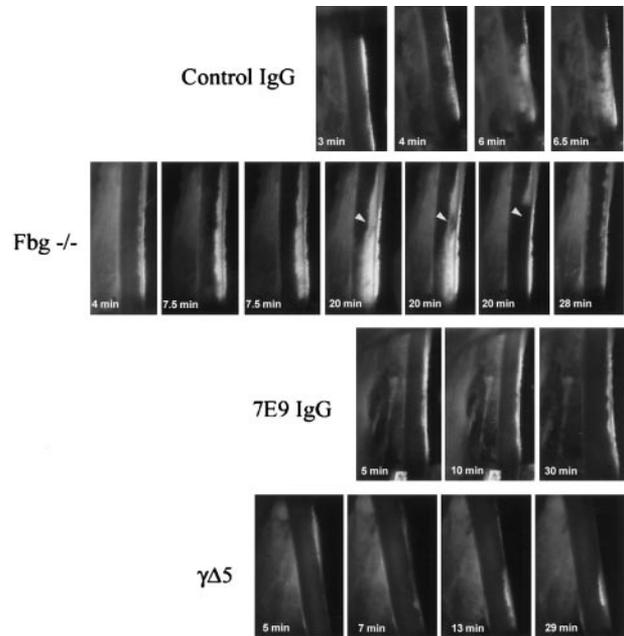

Figure 4. Dynamic demonstration of thrombus embolization in fbg$^{-/-}$ mice compared to control, 7E9-treated, and γΔ5 mice. Characteristics of thrombus growth after FeCl$_3$ injury. Single frames from the videos recorded through one eyepiece of the surgical microscope are shown, with blood flow proceeding from top to bottom. Thrombus formation at the site of the injury began rapidly in the mouse treated with control hamster IgG and the thrombus grew steadily more compact and dense without any significant macroscopic embolization. In the fbg$^{-/-}$ mouse, early platelet deposition was similar to that in the control mice, but the deposited platelets formed small loose thrombi that steadily embolized downstream from the site of the injury. Even though the thrombi at the site of the injury grew large, they were very unstable and repeatedly embolized. In the animal shown, a large, nearly occlusive thrombus formed after 20 minutes, but it soon began to stretch at one site (arrowhead) and then abruptly peeled off near its attachment to the vessel wall and embolized downstream. This particular embolus occluded the distal circulation, leading to transient cessation of blood flow. New thrombus deposition and additional embolization was visible at the site of injury 8 minutes later. Both 7E9-treated mice and γΔ5 mice differed dramatically from the control and fbg$^{-/-}$ mice in developing only small mural thrombi at the site of injury and only minimal embolization was observed. Original magnification × 15.

fbg$^{-/-}$ animals showed many large emboli occluding both the microvasculature and medium-size vessels. The emboli were more abundant and larger than those in any of the other animal groups (Figure 7).

7E9-treated mice. The pattern of thrombus formation in 7E9-treated mice (n = 9) was dramatically different from the pattern in the control and fbg$^{-/-}$ mice. The initial blood flow in the carotid arteries of 7E9-treated animals was about 30% lower than in the other animal groups (0.9 ± 0.5 mL/min versus 1.3 ± 0.3 mL/min; P = .04). Despite this, 7E9-treated mice developed only small

Table 2. Time to more than 90% reduction in blood flow after application of FeCl$_3$ in different groups of mice

Group (no. of mice)	No. mice with carotid artery occlusion within a given time				P versus control
	Less than 10 min	10-20 min	20-30 min	More than 30 min	
Control (14)	12	2	0	0	NA
Fbg$^{-/-}$ (7)	2*	0	1*	4	.001
7E9-treated (9)	0	1	0	8	< .0001
γΔ5 (4)	0	0	0	4	.0003

NA indicates not applicable.

*Reduction in flow due to distal embolization, not to occlusive thrombus at the site of injury.

Figure 5. Compared to control, fbg⁻/⁻ mice produce loosely packed large thrombi and both 7E9-treated and γΔ5 mice produce small mural thrombi. Scanning electron micrographs of carotid arteries of a control IgG-treated mouse, a fbg⁻/⁻ mouse, a 7E9-treated mouse, and γΔ5 mouse 30 minutes after FeCl₃ injury. There was a large, dense thrombus in the animal treated with control IgG, a large but loosely packed thrombus in the fbg⁻/⁻ animal, and smaller mural thrombi in both the γΔ5 mouse and 7E9-treated mouse.

Control IgG

Fbg -/-

γΔ5

7E9 IgG
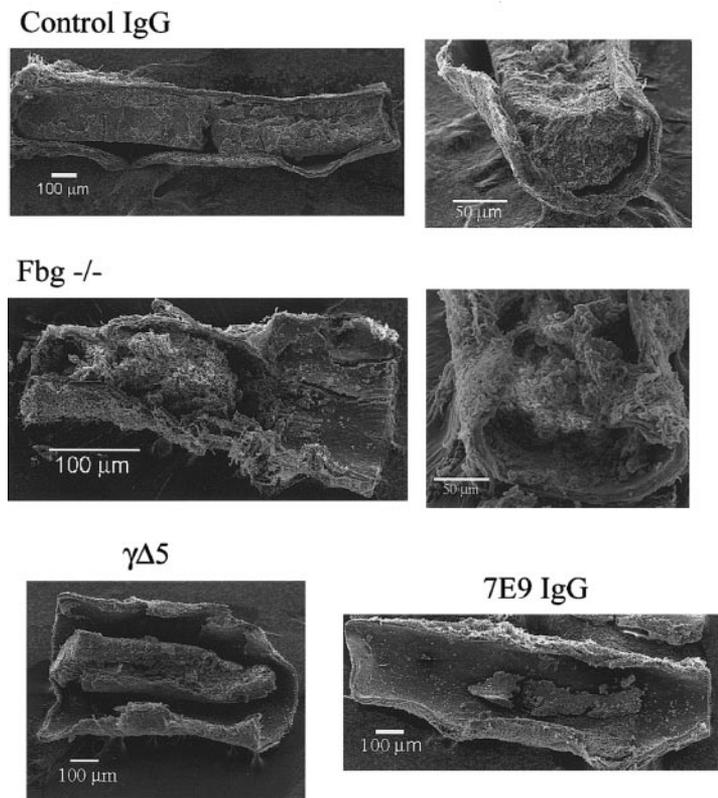
mural thrombi with little embolization (Figures 3D,5-6). Only one of the mice developed an occlusive thrombus that occurred after 11.3 minutes (Table 2). Thrombus formation began immediately after removal of filter paper with FeCl₃ but progressed at a slower rate than in the control animals. Some embolization was observed, greater than in control animals, but it consisted primarily of small emboli breaking off from the top of the growing thrombus. These emboli were much smaller than those formed in fbg⁻/⁻ mice and

the vessels did not occlude downstream from the site of injury (Figure 3D; Supplemental Video 3 contains details). In most cases the visible embolization stopped about 10 minutes after FeCl₃ application and then the thrombus stabilized (video C). The small mural thrombi that formed by 30 minutes after the injury were densely packed (Figures 5-6). These animals had few evident emboli within the brain vasculature, similar to that observed in control animals (Figure 7). Platelet counts at the end of the experiments did not differ significantly from those at the beginning ($1000 \pm 100 \times 10^3/\mu L$ before, $1000 \pm 200 \times 10^3/\mu L$ after).
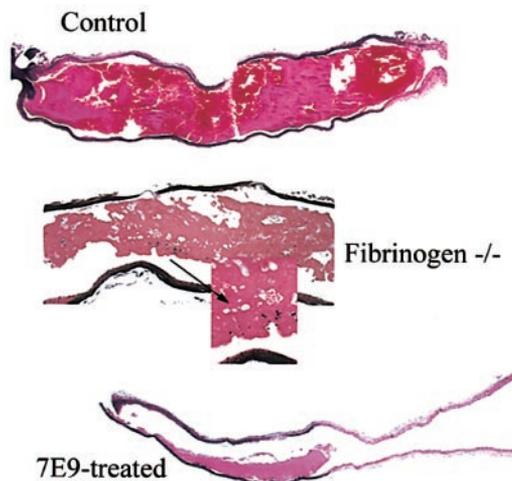

Control

Fibrinogen -/-

7E9-treated

Figure 6. Compared to control, fbg⁻/⁻ mice produce loosely packed thrombi with large pores and 7E9-treated mice produce small mural thrombi. Sections stained with hematoxylin and eosin from carotid artery segments obtained 30 minutes after FeCl₃-induced injury. Carotid sections from a control mouse (original magnification × 4), a fbg⁻/⁻ mouse (original magnifications × 10 and × 60), and a 7E9-treated mouse (original magnification × 4). Arrow shows unusually large pores observed only in thrombi of fbg⁻/⁻ animals.
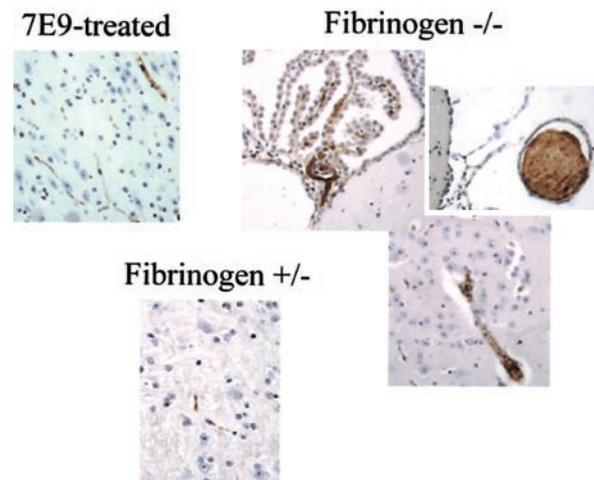

7E9-treated

Fibrinogen -/-

Fibrinogen +/-

Figure 7. Thrombus formation and embolization in the carotid arteries of fbg⁻/⁻ mice produce large emboli that occlude large blood vessels in the brain. Immunostaining of brain sections from animals at the end of the experiments with polyclonal antibody to mouse platelets revealed large emboli occluding vessels in brains of fbg⁻/⁻ animals when compared to the control fbg⁺/⁻ animal or 7E9-treated animal (original magnification × 20).

Mice expressing γΔ5. The pattern of thrombus formation in γΔ5 mice (n = 4) following FeCl$_3$ injury was similar to that of mice treated with 7E9 antibody. Thus, γΔ5 mice developed only small mural thrombi within the injured carotids (Figures 5-6) and in each case blood flow was maintained throughout the 30 minutes recording period (Table 2; Figure 3E). Thrombus formation began within the same timeframe as in control animals, but it progressed much more slowly. Embolization was greater than in control mice, but much less than in fbg$^{-/-}$ mice, resembling the embolization in 7E9-treated animals (Supplemental Video 4), with small emboli breaking off from the tops of the growing thrombi. Consistent with this finding, relatively few emboli were observed in the cerebral blood vessels of γΔ5 mice, similar to the pattern found in 7E9-treated animals (data not shown). The small mural thrombi formed 30 minutes after the injury were also comparable to those formed in 7E9-treated animals and were more densely packed than those in fbg$^{-/-}$ animals (Figures 5-6). Systemic platelet counts did not decrease significantly during the experiments ($800 \pm 200 \times 10^3/$μL before, $800 \pm 300 \times 10^3/$μL after).

Discussion

This study provides new insights into the relative contributions of different fibrinogen functions to large vessel thrombosis in the mouse. By adding intravital microscopy to our previous model[19] we were able to obtain real-time dynamic information. In addition, analysis of the distal circulation in the brain histologically enabled us to confirm the dynamic observations made regarding embolization of thrombi. The most remarkable and unexpected finding was that mice lacking the platelet recognition site at the C-terminus of the fibrinogen γ chain (γΔ5) and mice treated with antibody 7E9, which reacts with C-terminus of the fibrinogen γ chain, exhibited more limited thrombus formation and developed fewer and smaller emboli than fibrinogen-deficient mice with a complete lack of clotting function.

The thrombi that developed in the fbg$^{-/-}$ differed from those formed in wild-type control animals in several ways: (1) Instead of the gradual development of a tightly adherent thrombus in control mice, leading to vaso-occlusion at the site of injury within about 8 minutes, fbg$^{-/-}$ mice developed large, loosely packed thrombi that were not sufficiently secure to stably occlude the blood vessel at the site of injury. (2) Instead of the relatively infrequent embolization of small platelet aggregates from the growing thrombus surface of control animals, small to intermediate-sized platelet aggregates constantly embolized from the growing surface of the thrombi of fbg$^{-/-}$ mice. (3) Occasionally, very large thrombi broke off from the thrombi in fbg$^{-/-}$ mice, usually following the development of a tear in the thrombus that extended to near the vessel wall. The time to vessel occlusion was significantly prolonged in fbg$^{-/-}$ mice, with 4 of 7 animals failing to develop occlusive thrombi within the 30-minute time period of the experiment and 3 of 7 animals having cessation of blood flow at earlier time points due to distal embolization rather than thrombus formation at the site of injury. In sharp contrast, only small mural thrombi formed in γΔ5 and 7E9-treated mice, and embolization was limited in both the number and size of emboli. Only one in 9 of 7E9-treated and none of the γΔ5 animals developed occlusive thrombi or cessation of blood flow due to distal embolization during the entire length of the experiment (30 minutes).

Ni et al[10,11] previously studied FeCl$_3$-induced thrombus formation in mesenteric arterioles of wild-type, fbg$^{-/-}$, and γΔ5 mice.

They also found that large thrombi formed rapidly in fbg$^{-/-}$ mice and that the thrombi were unstable and repeatedly embolized downstream. Unlike the results in our experiments, they did not observe prolongation of the time to cessation of blood flow in fbg$^{-/-}$ mice, but consistent with our results, in all fbg$^{-/-}$ mice the cessation of blood flow was not due to obstruction at the site of injury, but rather due to obstruction of the distal microcirculation by emboli. The γΔ5 mice also produced thrombi rapidly, but unlike our results, in which none of the γΔ5 mice developed occlusive thrombi at the site of carotid artery injury, 88% of the animals developed thrombi that occluded the mesenteric arteriole at the site of injury. Embolization of thrombi in their model in the γΔ5 mice was greater than in control mice, but the emboli were noted to be released from the tops of the thrombi rather than from the bases, as was observed with the fbg$^{-/-}$ mice.

Our model differs from the mesenteric arteriole model primarily with regard to size of the blood vessel, blood flow through the vessel, and the capacitance of the downstream circulation. Thus, mesenteric arterioles are about 0.1 mm in diameter, whereas the carotid artery is about 0.5 mm. This 5-fold increase in diameter translates into a 25-fold increase in cross-sectional area, thus requiring greater thrombus size and stability to produce occlusion. Despite the difference in vessel size, the reported shear rates are similar at about 1300 to 1400 s^{-1}.[10] Thus, the differences in results with the γΔ5 mice between our study and that of Ni et al[10] probably reflect the inability of the thrombi in γΔ5 mice to grow much beyond 0.1 mm from the surface of the blood vessel. Also in contrast to the results obtained by Ni et al,[10] cessation of blood flow due to distal embolization only occurred in 3 of 7 fbg$^{-/-}$ mice in our study compared to all of the mice they studied. This difference probably reflects the greater capacity of the circulation distal to the carotid artery to remain patent in the face of extensive upstream embolization compared to the microcirculation distal to mesenteric arterioles. As a result, we were able to observe that all 4 fbg$^{-/-}$ mice that did not develop cessation of blood flow due to embolization failed to develop occlusive thrombi at the site of injury for the entire length of the experiment (30 minutes), compared to the control value of 8 ± 2 minutes. Thus, we believe that the apparent discrepancies between our findings and those of Ni et al[10,11] can be readily reconciled by considering the difference in the vascular injury models, especially in the size of the injured vessels, the blood flow through the vessels, and the characteristics of the downstream vasculature. In fact, the ability of γΔ5 mice to develop occlusive thrombi in small, but not large vessels, may help to explain the seemingly paradoxical observations of Holmback et al[15] that γΔ5 mice had markedly prolonged bleeding times in comparison to control animals following nail bed injury, but blood loss similar to that of control animals after surgical skin incisions.

Both scanning electron microscopy and histology of thrombi at the site of the injury revealed large, loosely packed thrombi in fbg$^{-/-}$ animals. These data are in accord with in vitro data demonstrating that platelet thrombi formed when afibrinogenemic blood is passed over vascular segments or collagen-coated surfaces at shear rates of 1500 s^{-1} or 2600 s^{-1} are large and loosely packed.[21-24] At a shear rate of 4500 s^{-1}, however, Tsuji et al[23] found that thrombi formed from normal blood continue to grow, whereas thrombi formed from afibrinogenemic blood begin to collapse, indicating their fragility and instability. Matsui et al[21] found dramatic spatial and temporal separations between von Willebrand factor (VWF) and fibrinogen antigen in thrombi formed from normal blood at a shear rate of 1500 s^{-1}. VWF was detected at the base and outside of the thrombi throughout the time of thrombus

development, whereas fibrinogen was exclusively found in the center of the thrombi and only at the later time points. These data indicate that fibrinogen is strategically located in the center of the thrombus where it is ideally situated to provide support against embolization as the thrombus grows in size over time. Clinical data also indicate that fibrinogen is not absolutely required for thrombus formation because a number of patients with afibrinogenemia have suffered venous or arterial thrombotic phenomena. Of particular note is that large embolic phenomena were documented in many of these patients.[25-27]

On the basis of a wealth of data, we speculate that the initial adhesion of platelets to the injured vessel wall is mediated primarily by VWF and the glycoprotein Ib-IX-V complex in fbg$^{-/-}$, fbg γΔ5, and 7E9-treated mice.[23,28] It is much less clear, however, which $\alpha_{IIb}\beta_3$ ligands support further thrombus development in each group of animals. Based on data in humans and mice, it appears that VWF can contribute to platelet thrombus formation as well as to platelet adhesion, especially when there is little or no fibrinogen to compete with the VWF for binding to $\alpha_{IIb}\beta_3$.[24,29-31] Ni et al[10,11] found that fbg$^{-/-}$ and γΔ5 mice have marked increases in platelet fibronectin and thus suggested that fibronectin may be an important $\alpha_{IIb}\beta_3$ ligand in these animals. Moreover, in vitro studies have demonstrated interactions between platelets and immobilized fibronectin[32] and recent evidence indicates that plasma fibronectin is important in thrombus formation in vivo in mice.[33] Nevertheless, our carotid artery injury studies indicate that an increase in platelet fibronectin, or platelet engagement of fibronectin, could not effectively compensate for the fibrinogen defect in γΔ5 mice.

There are several possible explanations for the observation that γΔ5 and 7E9-treated mice have smaller thrombi than mice lacking fibrinogen. The first is that γΔ5 fibrinogen and fibrinogen treated with 7E9 may act as inhibitors of thrombus growth and stabilization. Because fibrinogen is quickly deposited at the site of injury, it is possible that deposition of fibrin(ogen) molecules that cannot bind platelet integrin $\alpha_{IIb}\beta_3$ actually passivates the thrombus because they cannot recruit additional platelets. In the case of 7E9, some fibrinogen molecules may have only one 7E9 antibody bound to it. The one free γ chain could then bind to platelet $\alpha_{IIb}\beta_3$, but the blocked one could not bind to another $\alpha_{IIb}\beta_3$ on another platelets. In essence, such fibrinogen/7E9 complexes would act as $\alpha_{IIb}\beta_3$ antagonists. An alternative explanation for the difference in thrombus formation between the fbg$^{-/-}$ mice and the γΔ5 and 7E9-treated mice rests on the well-described ability of fibrin to bind thrombin and sequester it so that it is unavailable for acting in fluid phase.[6,34] This activity of fibrin was initially given the name antithrombin I.[7] Support for a significant biologic role for fibrin's ability to bind and sequester thrombin comes from (1) studies of select patients with dysfibrinogenemias such as New York 1, Milano II, and Naples I, whose fibrin did not bind thrombin normally and who developed venous or arterial thrombosis; (2) the previously indicated paradoxical finding of thrombosis in patients with afibrinogenemia and hypofibrinogenemia; (3) the presence of increased levels of prothrombin activation fragment $F_{1.2}$ and thrombin-antithrombin complexes in afibrinogenemic plasma; and (4) the ability of fibrinogen to normalize a number of the abnormalities described (for reviews, see Mosesson[7] and Hayes[9]).

In conclusion, our data demonstrate that the complexity of fibrinogen's prothrombotic and antithrombotic effects, the complexity of the multiple ligands that can bind to $\alpha_{IIb}\beta_3$, and the impact of blood vessel size on the results of murine models of thrombosis. All need to be carefully considered in developing safe and effective antithrombotic agents.

Acknowledgments

References

1. Lowe GD, Rumley A. Fibrinogen and its degradation products as thrombotic risk factors. Ann N Y Acad Sci. 2001;936:560-565.

2. Cheresh DA, Berliner SA, Vicente V, Ruggeri ZM. Recognition of distinct adhesive sites on fibrinogen by related integrins on platelets and endothelial cells. Cell. 1989;58:945-953.

3. Kloczewiak M, Timmons S, Hawiger J. Recognition site for the platelet receptor is present on the 15-residue carboxy-terminal fragment of the gamma chain of human fibrinogen and is not involved in the fibrin polymerization reaction. Thromb Res. 1983;29:249-255.

4. Doolittle RF, Chen R, Lau F. Hybrid fibrin: proof of the intermolecular nature of γ-γ cross-linking units. Biochem Biophys Res Commun. 1971;44: 94-100.

5. Yang Z, Mochalkin I, Doolittle RF. A model of fibrin formation based on crystal structures of fibrinogen and fibrin fragments complexed with synthetic peptides. Proc Natl Acad Sci U S A. 2000; 97:14156-14161.

6. de Bosch NB, Mosesson MW, Ruiz-Saez A, Echenagucia M, Rodriguez-Lemoin A. Inhibition of thrombin generation in plasma by fibrin formation (antithrombin I). Thromb Haemost. 2002;88: 253-258.

7. Mosesson MW. Antithrombin I: inhibition of thrombin generation in plasma by fibrin formation. Thromb Haemost. 2003;89:9-12.

8. Medved L, Nieuwenhuizen W. Molecular mechanisms of initiation of fibrinolysis by fibrin. Thromb Haemost. 2003;89:409-419.

9. Hayes T. Dysfibrinogenemia and thrombosis. Arch Pathol Lab Med. 2002;126:1387-1390.

10. Ni H, Denis CV, Subbarao S, et al. Persistence of platelet thrombus formation in arterioles of mice lacking both von Willebrand factor and fibrinogen. J Clin Invest. 2000;106:385-392.

11. Ni H, Papalia JM, Degen JL, Wagner DD. Control of thrombus embolization and fibronectin internalization by integrin $\alpha_{IIb}\beta_3$ engagement of the fibrinogen γ chain. Blood. 2003;102:3609-3614.

12. Jirouskova M, Smyth SS, Kudryk B, Coller BS. A hamster antibody to the mouse fibrinogen γ chain inhibits platelet-fibrinogen interactions and FXIIIa-mediated fibrin cross-linking, and facilitates thrombolysis. Thromb Haemost. 2001;86:1047-1056.

13. Scheiner T, Jirouskova M, Nagaswami C, Coller BS, Weisel JW. A monoclonal antibody to the fibrinogen γ chain alters fibrin clot structure and its properties by producing short, thin fibers arranged in bundles. J Thromb Haemost. 2003;1: 2594-2602.

14. Suh TT, Holmback K, Jensen NJ, et al. Resolution of spontaneous bleeding events but failure of pregnancy in fibrinogen-deficient mice. Genes Dev. 1995;9:2020-2033.

15. Holmback K, Danton MJ, Suh TT, Daugherty CC, Degen JL. Impaired platelet aggregation and sustained bleeding in mice lacking the fibrinogen motif bound by integrin $\alpha_{IIb}\beta_3$. EMBO J. 1996;15: 5760-5771.

16. Lengweiler S, Smyth SS, Jirouskova M, et al. Preparation of monoclonal antibodies to murine platelet glycoprotein IIb/IIIa ($\alpha_{IIb}\beta_3$) and other proteins from hamster-mouse interspecies hybridomas. Biochem Biophys Res Commun. 1999; 262:167-173.

17. Dejana E, Callioni A, Quintana A, de Gaetano G. Bleeding time in laboratory animals, II: a comparison of different assay conditions in rats. Thromb Res. 1979;15:191-197.

18. Hodivala-Dilke KM, McHugh KP, Tsakiris DA, et al. β_3-Integrin-deficient mice are a model for Glanzmann thrombasthenia showing placental defects and reduced survival. J Clin Invest. 1999; 103:229-238.

19. Smyth SS, Reis ED, Vaananen H, Zhang W, Coller BS. Variable protection of β_3-integrin-deficient mice from thrombosis initiated by different mechanisms. Blood. 2001;98:1055-1062.

20. Zhu Y, Carmeliet P, Fay WP. Plasminogen activator inhibitor-1 is a major determinant of arterial

thrombolysis resistance. Circulation. 1999;99: 3050-3055.

21. Matsui H, Sugimoto M, Mizuno T, et al. Distinct and concerted functions of von Willebrand factor and fibrinogen in mural thrombus growth under high shear flow. Blood. 2002;100:3604-3610.

22. Remijn JA, Wu YP, Ijsseldijk MJ, et al. Absence of fibrinogen in afibrinogenemia results in large but loosely packed thrombi under flow conditions. Thromb Haemost. 2001;85:736-742.

23. Tsuji S, Sugimoto M, Miyata S, et al. Real-time analysis of mural thrombus formation in various platelet aggregation disorders: distinct shear-dependent roles of platelet receptors and adhesive proteins under flow. Blood. 1999;94:968-975.

24. Weiss HJ, Hawiger J, Ruggeri ZM, et al. Fibrinogen-independent platelet adhesion and thrombus formation on subendothelium mediated by glycoprotein IIb-IIIa complex at high shear rate. J Clin Invest. 1989;83:288-297.

25. Dupuy E, Soria C, Molho P, et al. Embolized ischemic lesions of toes in an afibrinogenemic patient: possible relevance to in vivo circulating thrombin. Thromb Res. 2001;102:211-219.

26. Lak M, Keihani A, Elahi F, Peyvandi F, Mannucci PM. Bleeding and thrombosis in 55 patients with inherited afibrinogenaemia. Br J Haematol. 1999; 107:204-206.

27. Nilsson IM, Nilehn JE, Cronberg S, Norden G. Hypofibrinogenaemia and massive thrombosis. Acta Med Scand. 1966;180:65-76.

28. Savage B, Saldivar E, Ruggeri ZM. Initiation of platelet adhesion by arrest onto fibrinogen or translocation on von Willebrand factor. Cell. 1996; 84:289-297.

29. Denis C, Methia N, Frenette PS, et al. A mouse model of severe von Willebrand disease: defects in hemostasis and thrombosis. Proc Natl Acad Sci U S A. 1998;95:9524-9529.

30. Gralnick HR, Williams SB, Coller BS. Fibrinogen

competes with von Willebrand factor for binding to the glycoprotein IIb/IIIa complex when platelets are stimulated with thrombin. Blood. 1984;64: 797-800.

31. Schullek J, Jordan J, Montgomery RR. Interaction of von Willebrand factor with human platelets in the plasma milieu. J Clin Invest. 1984;73:421-428.

32. Beumer S, Ijsseldijk MJ, de Groot PG, Sixma JJ. Platelet adhesion to fibronectin in flow: dependence on surface concentration and shear rate, role of platelet membrane glycoproteins GP IIb/IIIa and VLA-5, and inhibition by heparin. Blood. 1994;84:3724-3733.

33. Ni H, Yuen PS, Papalia JM, et al. Plasma fibronectin promotes thrombus growth and stability in injured arterioles. Proc Natl Acad Sci U S A. 2003;100:2415-2419.

34. Liu CY, Nossel HL, Kaplan KL. The binding of thrombin by fibrin. J Biol Chem. 1979;254:10421-10425.